Output-feedback MPC for Robotic Systems under Bounded Noise

Lenka Kuklišová Pavelková[1][a] and Květoslav Belda[1][b]
[1]*The Czech Academy of Sciences, Institute of Information Theory and Automation*
Pod Vodárenskou věží 4, 182 08 Prague 8, Czech Republic
{pavelkov, belda}@utia.cas.cz

Keywords: Model predictive control, Output-feedback control, Robot manipulator, State estimation, Bayes methods, Bounded uncertainty

Abstract: The paper presents an output-feedback model predictive control applied to the motion control of a dynamic model of a parallel kinematic machine. The controlled system is described by a stochastic linear discrete-time model with bounded disturbances. An approximate uniform Bayesian filter provides set state estimates. The choice of the specific point estimate from this set is a part of the optimization. The cost function includes penalties on the tracking error and the actuation effort respecting increments. Illustrative examples show the effectiveness of the proposed approach and provide a comparison with previous results.

1 INTRODUCTION

The state-space formulation for model predictive control (MPC) is getting increased attention at industrial applications as the state-space model is suitable to describe the complex multi-input multi-output systems. The involved system states are often unmeasurable. Then, output-feedback MPC is suitable to solve the control problem mentioned above. Moreover, the controlled system is usually influenced by disturbances that are related to the model inaccuracy and to unmeasured noises. In many practical applications, these disturbances are only known to be bounded, and any additional information about their nature and properties is unavailable (Khlebnikov et al., 2011).

The output-feedback MPC that considers a bounded uncertainty is one of the recent research concerns. The state estimates can be obtained by the set-membership state estimation guaranteeing that the real system state lies in the bounded set (Qiu et al., 2020), (Brunner et al., 2018) or a specific robust Kalman filter can be used (Zenere and Zorzi, 2017). Recently, a tube-based robust MPC scheme, able to handle bounded noise was proposed (Mammarella and Capello, 2020), (Kögel and Findeisen, 2017).

In our research, we focus on the output-feedback MPC intended for industrial stationary robots-manipulators, specifically parallel kinematic machine (PKM) (Luces et al., 2017). Here, the system outputs are predominantly positions both longitudinal and angular. The relevant velocities correspond to unmeasured states, complemented possibly by accelerations. In this setting, measurements are often influenced by physically bounded uncertainties.

The previous paper of authors (Kuklišová Pavelková and Belda, 2019) deals with an output-feedback MPC for discrete-time systems influenced by bounded state and output disturbances. The control aim is to follow the reference trajectory that is known in advance. Point state estimates are obtained by a uniform Bayesian filter. The MPC design considers a quadratic cost function. The results are illustrated on a dynamic model of chosen PKM.

This paper extends the previous results (Kuklišová Pavelková and Belda, 2019) by considering set state estimate instead of the point state estimate and by using the incremental algorithm to reduce the control error.

Notation Matrices are in capital letters (e.g. A), vectors and scalars are in lowercase letters (e.g. b). A_{ij} is the element of a matrix A on i-th row and j-th column. A_i denotes the i-th row of A. We consider column vectors. z_t denotes the value of a vector variable z at a discrete-time instant $t \in \{1, \cdots, \bar{t}\}$; $z_{t;i}$ is the i-th entry of z_t; $\underline{z}$ and $\bar{z}$ are lower and upper bounds on z, respectively. $\hat{z}$ denotes the estimate of z. The symbol $f(\cdot|\cdot)$ denotes a conditional probability density function (pdf); names of arguments distinguish respective pdfs; no formal distinction is made

[a] https://orcid.org/0000-0001-5290-2389
[b] https://orcid.org/0000-0002-1299-7704

between a random variable, its realisation and an argument of the pdf. $\mathcal{U}_z(\underline{z},\overline{z})$ denotes a multivariate uniform distribution of z, $\underline{z} \le z \le \overline{z}$, inequalities are meant entrywise.

2 ROBOT MODEL

The chosen PKM, the redundant planar parallel robot-manipulator (Belda, 2010) is characterised by a four-dimensional input u (four torques) and a three-dimensional output y (tool center point (TCP) positions x_{TCP} and y_{TCP} and rotation angle φ_{TCP} of robot movable platform around the vertical axis), see Fig. 1.

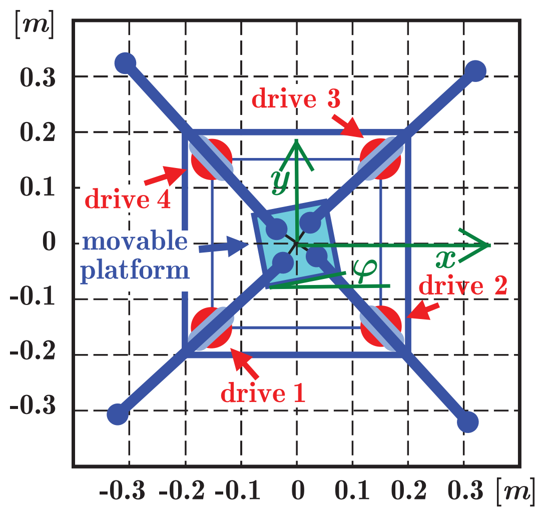

Figure 1: Wire frame model of robot.

The dynamics of the robot can be described by a set of non-linear differential equations representing equations of motion. They are composed using Lagrange equations (Belda et al., 2007)

$$\ddot{y} = \mathsf{f}(\dot{y}, y) + \mathsf{g}(y)\, u \qquad (1)$$

where $y = [\, x_{TCP},\ y_{TCP},\ \varphi_{TCP}]^T$. The corresponding non-linear continuous-time state-space model is defined as

$$\begin{bmatrix} \dot{y} \\ \ddot{y} \end{bmatrix} = \begin{bmatrix} \dot{y} \\ \mathsf{f}(\dot{y}, y) \end{bmatrix} + \begin{bmatrix} 0 \\ \mathsf{g}(y) \end{bmatrix} u \qquad (2)$$
$$y = \begin{bmatrix} I & 0 \end{bmatrix} \begin{bmatrix} y \\ \dot{y} \end{bmatrix}.$$

The nonlinear dynamics in (2) can be transformed into the linear-like form using a following linearizing decomposition (linearisation) (Valášek and Steinbauer, 1999)

$$\mathsf{f}(\dot{y}, y) = a_1(\dot{y}, y)\,\dot{y} + a_0(\dot{y}, y)\, y = \begin{bmatrix} \mathsf{f}_1(\dot{y}, y) \\ \mathsf{f}_2(\dot{y}, y) \\ \mathsf{f}_3(\dot{y}, y) \end{bmatrix}$$

$$\mathsf{f}(\dot{y}_r = 0, y_r = y_{\text{arbitrary}}) = 0 \qquad (3)$$

$$\mathsf{f}(\dot{y}, y) = \underbrace{\frac{\mathsf{f}(\dot{y}, y) - \mathsf{f}(0, y)}{.\dot{y}}}_{a_1(\dot{y}, y)}\, \dot{y} + \underbrace{\frac{\mathsf{f}(0, y) - \mathsf{f}(0, y_r)}{.y}}_{a_0(\dot{y}, y) = 0}\, y$$

where dot notation (symbol $\frac{*}{.*}$) in denominators means division element by element. The individual elements of $a_1(\dot{y}, y)$ are defined specifically as follows:

$$a_1(\dot{y}, y)\,\dot{y} =$$
$$\begin{bmatrix} \frac{\mathsf{f}_1(\dot{y},y) - \mathsf{f}_1(\dot{y}_x,y)}{\dot{x}} & \frac{\mathsf{f}_1(\dot{y}_x,y) - \mathsf{f}_1(\dot{y}_y,y)}{\dot{y}} & \frac{\mathsf{f}_1(\dot{y}_y,y) - \mathsf{f}_1(\dot{y}_\varphi,y)}{\dot{\varphi}} \\ \frac{\mathsf{f}_2(\dot{y},y) - \mathsf{f}_2(\dot{y}_x,y)}{\dot{x}} & \frac{\mathsf{f}_2(\dot{y}_x,y) - \mathsf{f}_2(\dot{y}_y,y)}{\dot{y}} & \frac{\mathsf{f}_2(\dot{y}_y,y) - \mathsf{f}_2(\dot{y}_\varphi,y)}{\dot{\varphi}} \\ \frac{\mathsf{f}_3(\dot{y},y) - \mathsf{f}_3(\dot{y}_x,y)}{\dot{x}} & \frac{\mathsf{f}_3(\dot{y}_x,y) - \mathsf{f}_3(\dot{y}_y,y)}{\dot{y}} & \frac{\mathsf{f}_3(\dot{y}_y,y) - \mathsf{f}_3(\dot{y}_\varphi,y)}{\dot{\varphi}} \end{bmatrix} \begin{bmatrix} \dot{x} \\ \dot{y} \\ \dot{\varphi} \end{bmatrix} \qquad (4)$$

$\dot{y}_x = [0, \dot{y}, \dot{\varphi}]^T$, $\dot{y}_y = [0, 0, \dot{\varphi}]^T$ and $\dot{y}_\varphi = [0, 0, 0]^T$. Note that $a_0(\dot{y}, y) = 0$ due to properties of the function $\mathsf{f}(\dot{y}, y)$.

After the decomposition, a linear time-varying (LTV) state-space model of robot can be written as follows

$$\dot{x} = A_c\, x + B_c\, u \qquad (5)$$

$$y = C\, x \qquad (6)$$

where $x = \begin{bmatrix} y & \dot{y} \end{bmatrix}^T$, $A_c = \begin{bmatrix} 0 & I \\ a_0(\dot{y}, y) & a_1(\dot{y}, y) \end{bmatrix}$, $B_c = \begin{bmatrix} 0 \\ \mathsf{g}(y) \end{bmatrix}$, $C = \begin{bmatrix} I & 0 \end{bmatrix}$. Using standard time discretisation and considering additive bounded disturbances, the following discrete-time linear state-space model (LSU model) is obtained

$$x_t = \underbrace{A_t\, x_{t-1} + B_t\, u_{t-1}}_{\tilde{x}_t} + \nu_t, \quad \nu_t \sim \mathcal{U}_\nu(-\rho, \rho) \qquad (7)$$

$$y_t = \underbrace{C x_t}_{\tilde{y}_t} + n_t, \qquad n_t \sim \mathcal{U}_n(-r, r) \qquad (8)$$

where $A_t = e^{A_c T_s}$, $B_t = \int_{t T_s}^{t T_s + T_s} e^{A_c (t T_s + T_s - \tau)} B_c \, \mathrm{d}\tau$; $\tilde{x}_t$ and $\tilde{y}_t$ correspond to the nominal values of x_t and y_t; ν_t and n_t are independent and identically distributed (i.i.d.) state and observation disturbances, they are uniformly distributed within an orthotope with known bounds ρ and r, respectively.

3 BAYESIAN STATE ESTIMATION OF LSU MODEL

Within the considered Bayesian framework (Kárný et al., 2005), a controlled system is described by:

$$\begin{aligned} \text{time evolution model:} \quad & f(x_t|x_{t-1},u_{t-1}) && (9)\\ \text{observation model:} \quad & f(y_t|x_t) && (10)\\ \text{prior pdf:} \quad & f(x_0) && (11) \end{aligned}$$

Bayesian state estimation (filtering) consists in the evolution of the posterior pdf $f(x_t|d(t))$ where $d(t)$ is a sequence of observed data records $d_t = (y_t,u_t)$, $d_0 \equiv u_0$. The evolution of posterior pdf $f(x_t|d(t))$ is described by a two-steps recursion that starts from the prior pdf $f(x_0|u_0) \equiv f(x_0)$ (11): (i) *time update* that uses theoretical knowledge described by model (9) and reflects the evolution $x_{t-1} \to x_t$; it provides prediction $f(x_t|d(t-1))$, and (ii) *data update* that uses theoretical knowledge described by model (10) and incorporates information about data d_t; it provides $f(x_t|d(t))$.

The LSU model (7), (8) can be equivalently described, using pdf notation (9)–(11), as follows

$$\begin{aligned} f(x_t|u_{t-1},x_{t-1}) &= \mathcal{U}_x(\tilde{x}_t-\rho,\tilde{x}_t+\rho) && (12)\\ f(y_t|x_t) &= \mathcal{U}_y(\tilde{y}_t-r,\tilde{y}_t+r) && (13)\\ f(x_0) &= \mathcal{U}_x(\underline{x}_0,\overline{x}_0) && (14) \end{aligned}$$

The exact solution of the Bayesian filtering of LSU model (12), (13) leads to a very complex form of posterior pdf. Recently, an approximate Bayesian state estimation of this model was proposed by one of authors (Jirsa et al., 2020). It provides the evolution of the uniformly distributed posterior pdf $f(x_t|d(t))$ as follows.

Time update – The time update starts at $t=1$ with $\underline{m}_0 = \underline{x}_0$, $\overline{m}_0 = \overline{x}_0$ and it holds

$$f(x_t|d(t-1)) \approx \prod_{i=1}^{\ell} \mathcal{U}_{x_{t;i}}(\underline{m}_{t;i}-\rho_i,\overline{m}_{t;i}+\rho_i) = \\ = \mathcal{U}_{x_t}(\underline{m}_t-\rho,\overline{m}_t+\rho), \quad (15)$$

where $\underline{m}_t = [\underline{m}_{t;1},\ldots,\underline{m}_{t;\ell}]'$, $\overline{m}_t = [\overline{m}_{t;1},\ldots,\overline{m}_{t;\ell}]'$, ℓ is the size of x,

$$\underline{m}_{t;i} = \sum_{j=1}^{\ell} \min(A_{ij}\underline{x}_{t-1;j}+B_i u_{t-1},A_{ij}\overline{x}_{t-1;j}+B_i u_{t-1}), \quad (16)$$

$$\overline{m}_{t;i} = \sum_{j=1}^{\ell} \max(A_{ij}\underline{x}_{t-1;j}+B_i u_{t-1},A_{ij}\overline{x}_{t-1;j}+B_i u_{t-1}).$$

Data update – In data update step, the observation y_t (13) is processed as $y_t - r \le Cx_t \le y_t + r$ by the Bayes rule together with the prior (15) from the time update. The resulting uniform pdf posses a support in the form of polytope. It is approximated by a uniform pdf with an orthotopic support

$$f(x_t|d(t)) \approx \mathcal{U}_{x_t}(\underline{x}_t,\overline{x}_t). \quad (17)$$

The proposed approximation is based on a minimising of Kullback-Leibler divergence of two pdfs (Jirsa et al., 2020).

The result of the approximate Bayesian filtering (17) says that the state estimate $\hat{x}_t$ lies within a set

$$\hat{x}_t \in \langle \underline{x}_t,\overline{x}_t \rangle \quad (18)$$

where all points have the same probability. In the previous paper of authors (Kuklišová Pavelková and Belda, 2019), the point state estimate for control algorithm was chosen to correspond to the centre of the orthotope in (17)

$$\hat{x}_t = \frac{\underline{x}_t+\overline{x}_t}{2}. \quad (19)$$

Here, we integrate the choice of point estimate into the optimisation step of control design.

4 CONTROL DESIGN

This section introduces two algorithms of output-feedback MPC, namely the positional and the incremental algorithm. To design an optimal control action, MPC employs predictions of expected future outputs of controlled system represented by a state space model. The main design elements, i.e. equations of predictions and relevant quadratic cost function are introduced in the following subsections.

4.1 Predictions of Future Outputs

The equations of predictions express the relationship between future predicted outputs and unknown control actions. They are composed using current state estimate in nominal parts of model (7) and (8). For simplicity, we omit here the time indices, i.e., $A_t \to A$ and $B_t \to B$, as for one optimisation step, the matrices are constant for whole prediction horizon N.

Prediction equations for the *positional control algorithm* (Kuklišová Pavelková and Belda, 2019) are composed as follows

$$\hat{Y}_{t+1} = \left[\hat{y}_{t+1}^T, \cdots, \hat{y}_{t+N}^T\right]^T = F_1\hat{x}_t + G_1 U_t, \\ U_t = \left[u_t^T, \cdots, u_{t+N-1}^T\right]^T \quad (20)$$

where

$$F_1 = \begin{bmatrix} CA \\ \vdots \\ CA^{N-1} \\ CA^N \end{bmatrix}, G_1 = \begin{bmatrix} CB & 0 & \cdots & 0 \\ \vdots & \ddots & \ddots & \vdots \\ CA^{N-2}B & \cdots & CB & 0 \\ CA^{N-1}B & \cdots & CAB & CB \end{bmatrix}.$$

To achieve integral property in the design, the nominal parts of model (7) and (8) are rewritten in incremental forms as follows

$$\begin{aligned} \Delta\hat{x}_{t+1} &= \hat{x}_{t+1} - \hat{x}_t = A\,\Delta\hat{x}_t + B\,\Delta u_t \\ \Delta\hat{y}_{t+1} &= \hat{y}_{t+1} - y_t = C\,\Delta\hat{x}_{t+1}. \end{aligned} \tag{21}$$

The prediction equations for *incremental control algorithm* are composed recursively using the model (21). The recursivity is involved by the index $j = 1, \cdots, N$ that determines individual discrete time instants for the horizon N,

$$\Delta\hat{x}_{t+j} = A^j\,\Delta\hat{x}_t + \sum_{i=1}^{j} A^{i-1} B \Delta u_{t+j-i} \tag{22}$$

$$\Delta\hat{y}_{t+j} = CA^j\,\Delta\hat{x}_t + \sum_{i=1}^{j} CA^{i-1} B \Delta u_{t+j-i} \tag{23}$$

The evolution of the full-value predictions of the system outputs $\hat{y}$ is

$$\hat{y}_{t+j} = y_t + \sum_{i=1}^{j} \Delta\hat{y}_{t+i} \tag{24}$$

The relevant matrix notation of (24) is as follows

$$\hat{Y}_{t+1} = F_I\,y_t + F_2\,\Delta\hat{x}_t + G_2\,\Delta U_t \tag{25}$$

where

$$\hat{Y}_{t+1} = [\ \hat{y}_{t+1}^T \ \cdots \ \hat{y}_{t+N}^T\ ]^T, F_I = [\ I \ \cdots \ I\ ]^T,$$

$$F_2 = \begin{bmatrix} CA \\ \vdots \\ \sum_{i=1}^{N} CA^i \end{bmatrix}, G_2 = \begin{bmatrix} CB & \cdots & 0 \\ \vdots & \ddots & \vdots \\ \sum_{i=1}^{N} CA^{i-1}B & \cdots & CB \end{bmatrix}$$

4.2 Cost Function

The behaviour of a control process is influenced by the choice of the cost function. We use a quadratic cost function. It balances control errors, i.e. differences between predicted outputs and reference values, against amount of input energy given by control vector or control increments, respectively.

The cost function for the *positional algorithm* (Kuklišová Pavelková and Belda, 2019) is

$$J_t = \sum_{j=1}^{N} \left\{ \|Q_{yw}(\hat{y}_{t+j} - w_{t+j})\|_2^2 + \|Q_u u_{t+j-1}\|_2^2 \right\} \tag{26}$$

The cost function for the *incremental algorithm* is

$$J_t = \sum_{j=1}^{N} \left\{ \|(Q_{yw}(\hat{y}_{t+j} - w_{t+j})\|_2^2 + \left\|Q_{\Delta u} \Delta u_{t+j-1}\right\|_2^2 \right\} \tag{27}$$

where $\|.\|_2^2$ means the squared Euclidean norm.

4.3 Minimization Procedure

Optimality criterion is defined as follows

$$\min_{\mathbb{U}_t} J_t(\hat{Y}_{t+1}, W_{t+1}, \mathbb{U}_t),\ \mathbb{U}_t \in \{U_t, \Delta U_t\} \tag{28}$$

s.t. state space model (7) and (8)
set state estimate $\hat{x}_t$ (18)

where $\hat{Y}_{t+1}$ are prediction equations (20) or (25), respectively, W_{t+1} represents a sequence of references

$$W_{t+1} = \left[w_{t+1}^T, \cdots, w_{t+N}^T\right]^T \tag{29}$$

The involved cost function J_t (26) or (27) are rewritten into the square-root form

$$J_t = \mathbb{J}_t^T \mathbb{J}_t \tag{30}$$

Positional algorithm

The square-root $\mathbb{J}_t$ of the cost function J_t (30) is

$$\begin{aligned} \mathbb{J}_t &= \begin{bmatrix} Q_{YW} & 0 \\ 0 & Q_U \end{bmatrix} \begin{bmatrix} \hat{Y}_{t+1} - W_{t+1} \\ U_t \end{bmatrix} \\ &= \begin{bmatrix} Q_{YW} F \hat{x}_t + Q_{YW} G U_t - Q_{YW} W_{t+1} \\ Q_U U_t \end{bmatrix}. \end{aligned} \tag{31}$$

where Q_{YW}, $Q_{\Delta U}$ and Q_U are penalisation matrices defined as follows

$$Q_\diamond^T Q_\diamond = \begin{bmatrix} Q_*^T Q_* & & 0 \\ & \ddots & \\ 0 & & Q_*^T Q_* \end{bmatrix} \left| \begin{array}{l} \text{subscripts } \diamond, *: \\ \diamond \in \{YW, \Delta U, U\} \\ * \in \{yw, \Delta u, u\} \end{array} \right. \tag{32}$$

Considering minimization of the square-root $\mathbb{J}_t$ as a specific solution of least-squares problem leads to the following algebraic equation (Kuklišová Pavelková and Belda, 2019):

$$\begin{bmatrix} Q_{YW} G & Q_{YW}(W_{t+1} - F\hat{x}_t) \\ Q_U & 0 \end{bmatrix} \begin{bmatrix} U_t \\ -I \end{bmatrix} = 0 \tag{33}$$

Incremental algorithm
The square-root $\mathbb{J}_t$ of the cost function J_t (30) is

$$\mathbb{J}_t = \begin{bmatrix} Q_{YW} & 0 \\ 0 & Q_{\Delta U} \end{bmatrix} \begin{bmatrix} \hat{Y}_{t+1} - W_{t+1} \\ \Delta U_t \end{bmatrix}$$
$$= \begin{bmatrix} Q_{YW}\left(F_I\, y_t + F_2 \Delta x_t + G_2\, \Delta U_t - W_{t+1}\right) \\ Q_{\Delta U} \Delta U_t \end{bmatrix}. \quad (34)$$

Considering minimization of the square-root $\mathbb{J}_t$ as a specific solution of least-squares problem leads to the following algebraic equation:

$$\begin{bmatrix} Q_{YW}\, G_2 & Q_{YW}\, Z \\ Q_{\Delta U} & 0 \end{bmatrix} \begin{bmatrix} \Delta U_t \\ -I \end{bmatrix} = 0 \quad (35)$$

with $Z = W_{t+1} - F_I\, y_t - F_2\, \Delta x_t$.

The over-determined system (33) or (35), respectively, can be rewritten into the condensed general form $\mathcal{A}\, \mathbb{U}_t = b$.

This form can be transformed by orthogonal-triangular decomposition (Lawson and Hanson, 1995) into the following form and solved for unknown $\mathbb{U}_t$

$$Q^T \mathcal{A}\, \mathbb{U}_t = Q^T b \;\; \text{assuming that} \;\; \mathcal{A} = QR$$
$$R_1\, \mathbb{U}_t = c_1 \quad (36)$$

where $\mathbb{U}_t \in \{U_t, \Delta U_t\}$, Q^T is an orthogonal matrix that transforms matrix $\mathcal{A}$ into upper triangle R_1.

It is indicated by the following equation diagram

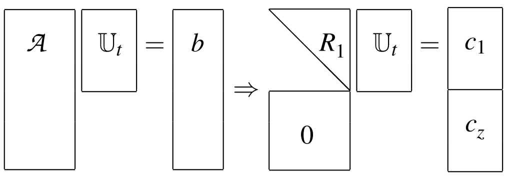

(37)

Vector c_z represents a loss vector. Euclidean norm $||c_z||_2$ corresponds to the square-root of the minimum of cost function (26) or (27), i.e., $J_t = c_z^T c_z$.

In the previous paper of authors (Kuklišová Pavelková and Belda, 2019), the transformation into (36) was performed once using the point state estimate (19).

Here, we consider the set estimate (18). The transformation into (36) is performed successively for properly selected points from the whole set. Subsequently, the realisation with the minimal value of $||c_z||_2$ is chosen as the result.

For control, only the first elements corresponding to u_t are used from computed vector $\mathbb{U}_t$. Then, for the *positional algorithm*

$$u_t = M U_t \quad (38)$$

and for the *incremental algorithm*

$$u_t = u_{t-1} + M\, \Delta U_t \quad (39)$$

where matrix M is defined as $M = [I_{n_u}, 0_{n_u}, \cdots, 0_{n_u}]$, n_u is dimension of vector of control actions u_t.

Algorithmic summary
The following summary describes a sequence performed during the control process.

Initialisation:

i. set the initial state $\hat{x}_0 \in \langle \underline{x}_0, \overline{x}_0 \rangle$ and control u_0
ii. set $t := 1, \bar{t} \geq 1$
iii. load the reference trajectory $w_1, w_2, \ldots, w_{\bar{t}}$
iv. initialise nonlinear continuous model (1)
v. set r and ρ for LSU model (7) and (8)
vi. set N, Q_* in (26) or (27), respectively

On-line phase:

1. update the model matrices A_t, B_t in (7) and (8)
2. select representative points from the set (18)
3. compute c_z (37) for selected points
4. choose the control input u_t (38) or (39) that corresponds to minimal $||c_z||_2$
5. simulate a new state of model (1) in $t+1$
6. set time $t := t+1$
7. measure disturbed system output y_t
8. obtain the set state estimate $\hat{x}_t \in \langle \underline{x}_t, \overline{x}_t \rangle$ (18)
9. if $t < \bar{t}$, go to 1.

End, result evaluation.

5 EXPERIMENTS

This section demonstrates the proposed output-feedback MPC applied to the motion control of PKM robot depicted in Figure 1 represented by the model of the machine dynamics. It is described in Sec. 'Robot model', specifically by the equations (1)-(8).

5.1 Experiment Setup

The real controlled system, as depicted in Figure 2 on the left, is simulated by (1) with an added uniform noise. The testing trajectory is depicted in Figure 2 on the right.

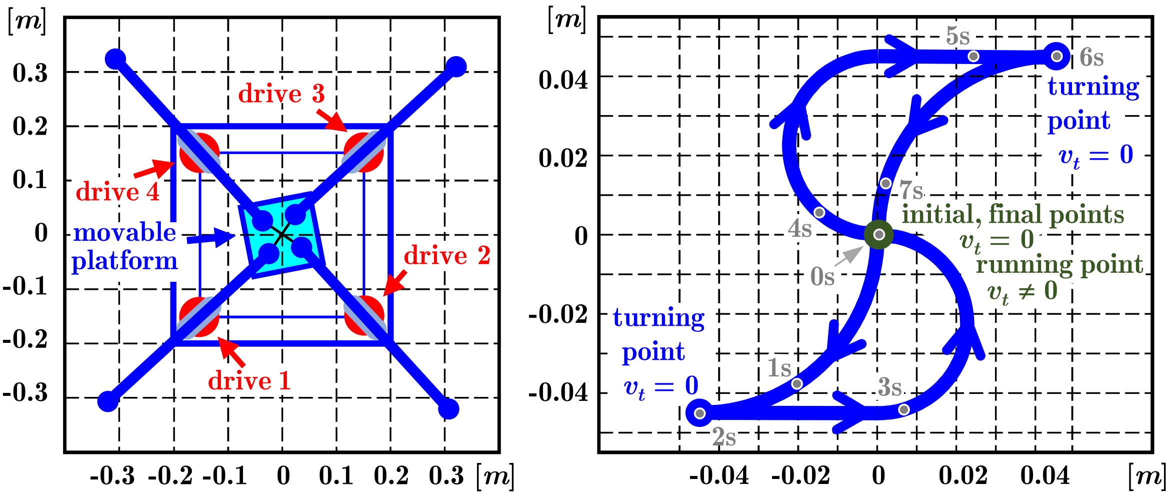

Figure 2: Considered robot 'Moving Slide' and used testing trajectory.

The state estimates $\hat{x}_t \in \langle \underline{x}_t, \overline{x}_t \rangle$ (18) are obtained using the model (7) and (8) with the noise bounds set as follows: $\rho = 10^{-6}[m, m, rad, m\,s^{-1}, m\,s^{-1}, rad\,s^{-1}]^T$, $r = 10^{-3}[m, m, rad]^T$. The control parameters in (26) or (27) are set as follows: $N = 10$; $Q_{yw} = I$, $Q_u = 10^{-2}I$, $Q_{\Delta u} = 2.5 \cdot 10^{-5}I$, where I is the identity matrix of the appropriate order.

The quality of the control process is evaluated by the visual comparison of the results and by the root mean square error (*RMSE*) between outputs y_t and references w_t

$$RMSE_i = \sqrt{\frac{1}{\bar{t}} \sum_{t=1}^{\bar{t}} (y_{t;i} - w_{t;i})^2}, \; i = \{1, 2, 3\}. \quad (40)$$

The following experiments were performed for the robot motion along the reference trajectory as depicted in Figure 2:

	control algorithm	state estimate
Exp. 1	positional (38)	point (19)
Exp. 2	positional (38)	set (18)
Exp. 3	incremental (39)	point (19)
Exp. 4	incremental (39)	set (18)

5.2 Results and Discussion

The results of individual experiments are shown in Figures 3–8. Figure 3 and Figure 4 show time histories for the positional algorithm. The positional algorithm with set state estimate (Exp. 2) reaches smaller dispersion control errors. Control errors do not tend to zero since both experiments Exp. 1 and Exp. 2 were realized with positional algorithm that has proportional character only. It is useful for fast repeated manipulation motion that does not need track the reference trajectory or stay in one position precisely but with smaller dynamic demands on robot drives.

Figure 5 shows the values $||c_z||_2$ in (37) for the positional algorithm (38) and the state estimate set (18) in the selected times, namely 1s, 2s, 3s, 4s, 5s and 6s. Filled blue circle indicates the searched cost function minimum that is used for the control design in accord with (37).

Figure 6 and Figure 7 show time histories for the incremental algorithm. The incremental algorithm with set state estimate (Exp. 4) reaches smaller dispersion control errors again. Control errors do not tend to zero, but they are symmetrically distributed around horizontal axis x since both experiments Exp. 1 and Exp. 2 were realized with incremental algorithm that push controlled system towards zero. However, due to noise, it is asymptotic trend.

Figure 8 shows the values $||c_z||_2$ in (37) for the incremental algorithm (39) and the state estimate set (18) in the selected times, namely 1s, 2s, 3s, 4s, 5s and 6s. Filled blue circle indicates the searched cost function minimum that is used for the control design in accord with (37).

The numerical comparison of $RMSE_i$ values for experiments Exp.1 – Exp.4 is presented in Table 1. The results are comparable. However, the optimisation in Exp. 2 and Exp. 4 takes into account cost values that balance not only control error but also magnitudes of control actions or their increments.

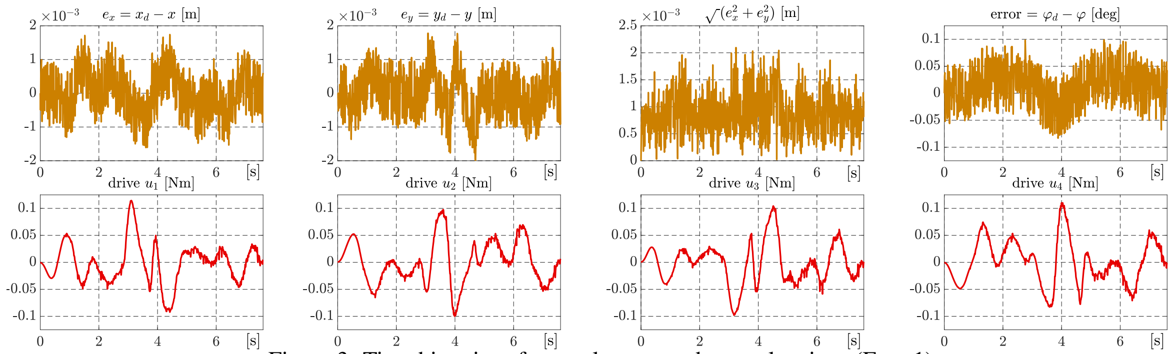

Figure 3: Time histories of control errors and control actions (Exp. 1).

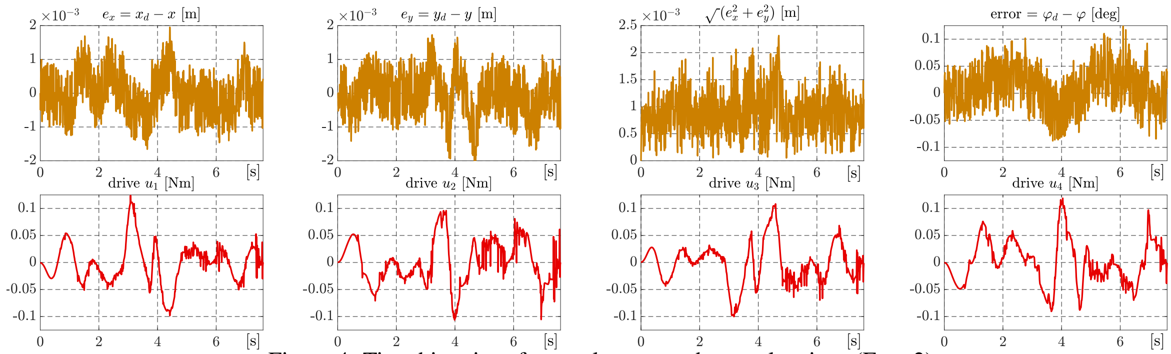

Figure 4: Time histories of control errors and control actions (Exp. 2).

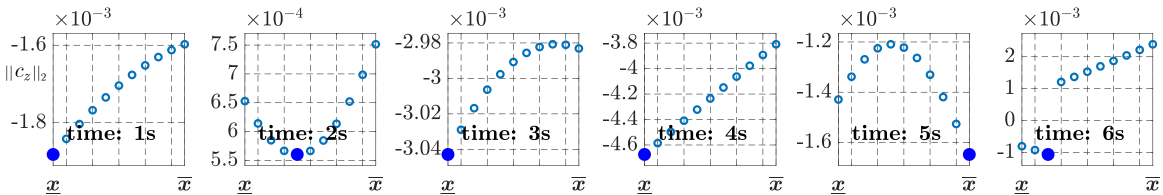

Figure 5: Selected time instants with the cost function for the set state estim. (Exp. 2).

Table 1: *RMSE$_i$* (40) for the individual experiments Exp. 1–Exp. 4.

	RMSE$_1$	*RMSE*$_2$	*RMSE*$_3$
Exp. 1	$0.694 \cdot 10^{-3}$	$0.705 \cdot 10^{-3}$	$0.705 \cdot 10^{-3}$
Exp. 2	$0.694 \cdot 10^{-3}$	$0.721 \cdot 10^{-3}$	$0.731 \cdot 10^{-3}$
Exp. 3	$0.622 \cdot 10^{-3}$	$0.633 \cdot 10^{-3}$	$0.669 \cdot 10^{-3}$
Exp. 4	$0.626 \cdot 10^{-3}$	$0.644 \cdot 10^{-3}$	$0.678 \cdot 10^{-3}$

6 CONCLUSION

The paper proposes a novel solution to the output-feedback MPC under bounded state and output disturbances. Comparing to the previous work of author (Kuklišová Pavelková and Belda, 2019), the proposed algorithm enables further reduction of the involved cost function (28) by considering set state estimates (18) and their inclusion into the minimization step. The selection of a suitable points from (18) is made by the user.

The proposed solution considers an unconstrained positional and incremental MPC. The overshoot of possible constraints is prevented by the appropriate design of reference trajectory and its suitable time parametrisation (Belda and Novotný, 2012).

The presented research is important for mechanical systems where bounded noises are present frequently but usually modelled by unbounded Gaussian distribution. In practice, the use of unbounded noises leads to over-conservative design, which induces a remarkable increase in the costs. The stochastic models built on bounded noises prevent these problems (d'Onofrio, 2013).

Next research will try to formulate the optimal selection of the points from the set (18). Also, a more flexible sets of estimates will be considered, namely zonotopes (Combastel, 2015), that will provide the less conservative guaranteed estimates comparing to the currently used orthotopic set.

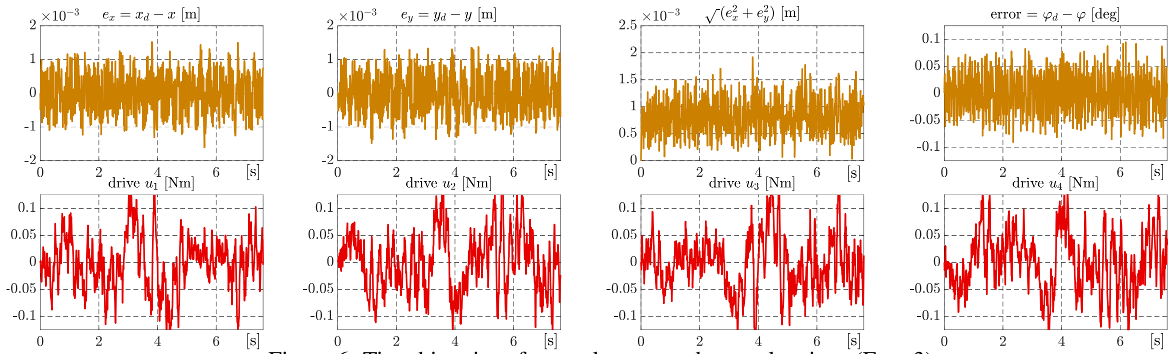

Figure 6: Time histories of control errors and control actions (Exp. 3).

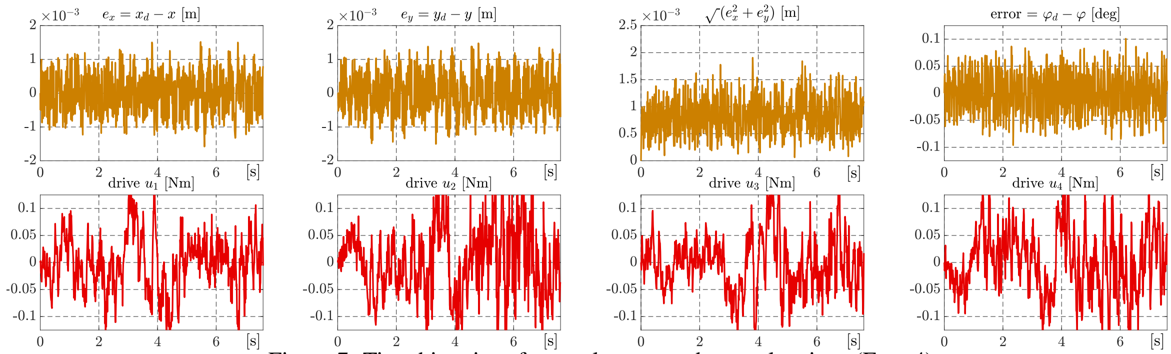

Figure 7: Time histories of control errors and control actions (Exp. 4).

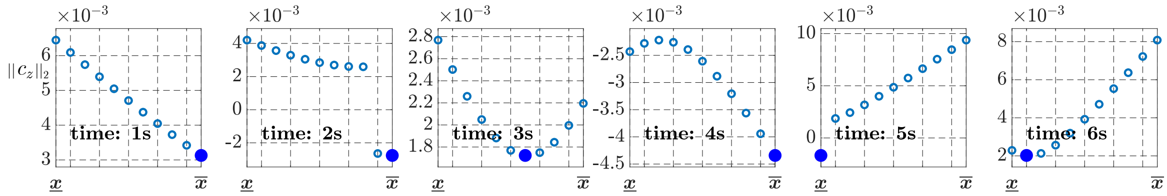

Figure 8: Several time instants with the cost function for the set state estim. (Exp. 4).

REFERENCES

Belda, K. (2010). Robotic device, Ct. 301781 CZ, Ind. Prop. Office.

Belda, K., Böhm, J., and Píša, P. (2007). Concepts of model-based control and trajectory planning for parallel robots. In Klaus, S., editor, *Proc. of 13th IASTED Int. Conf. on Robotics and Applications*, pages 15–20. Acta Press.

Belda, K. and Novotný, P. (2012). Path simulator for machine tools and robots. In *Proc. of the 17th Int. Conf. on Methods and Models in Automation and Robotics*, pages 373–378.

Brunner, F. D., Müller, M. A., and Allgöwer, F. (2018). Enhancing output-feedback mpc with set-valued moving horizon estimation. *IEEE Transactions on Automatic Control*, 63(9):2976–2986.

Combastel, C. (2015). Zonotopes and kalman observers: Gain optimality under distinct uncertainty paradigms and robust convergence. *Automatica*, 55:265–273.

d'Onofrio, A. (2013). *Bounded Noises in Physics, Biology, and Engineering*. Springer.

Jirsa, L., Kuklišová Pavelková, L., and Quinn, A. (2020). Approximate Bayesian prediction using state space model with uniform noise. In *Informatics in Control Automation and Robotics*, volume 613 of *LNEE*, pages 552–568. Springer.

Kárný et al. (2005). *Optimized Bayesian Dynamic Advising: Theory and Algorithms*. Springer.

Khlebnikov, M. V., Polyak, B. T., and Kuntsevich, V. M. (2011). Optimization of linear systems subject to bounded exogenous disturbances: The invariant ellipsoid technique. *Automation and Remote Control*, 72(11):2227–2275.

Kögel, M. and Findeisen, R. (2017). Robust output feedback MPC for uncertain linear systems with reduced conservatism. *IFAC-PapersOnLine*, 50(1):10685 – 10690.

Kuklišová Pavelková, L. and Belda, K. (2019). Output-feedback model predictive control for systems under uniform disturbances. In *2020 7th International Conference on Control, Decision and Information Technologies (CoDIT)*, pages 897–902.

Lawson, C. and Hanson, R. (1995). *Solving least squares problems*. Siam.

Luces, M., Mills, J. K., and Benhabib, B. (2017). A Review of Redundant Parallel Kinematic Mechanisms. *Journal of int. & robot. systems*, 86(2):175–198.

Mammarella, M. and Capello, E. (2020). Tube-Based Robust MPC Processor-in-the-Loop Validation for Fixed-Wing UAVs. *Journal of int. & robot. systems*, 100(1):239–258.

Qiu, Q., Yang, F., Zhu, Y., and Mousavinejad, E. (2020). Output feedback model predictive control based on set-membership state estimation. *IET Control Theory Applications*, 14(4):558–567.

Valášek, M. and Steinbauer, P. (1999). Nonlinear control of multibody systems. In *Proc. of Euromech*, pages 437–444.

Zenere, A. and Zorzi, M. (2017). Model Predictive Control meets robust Kalman filtering. *IFAC-PapersOnLine*, 50(1):3774–3779.